Using magnetic nano Fe^{n+}@GO as an efficient heterogeneous Fenton catalyst for the removal of tetracycline

Yuanxiu Yang[a], Chuang Yao[a],*, Junyuan Rao[a], Yuansheng Tang[a], Hui Liu[b], Xinjiang Hu[c], Jianxin Liu[a], Xian Huang[a], Hui Wang[d], Huankai Li[b]

[a]*Institute of Engineering Technology of Guangdong Province, Guangzhou, China, Tel. +86-020-8632-4662, email: 1107135727@qq.com (Y. Yang), yaochuang1984@163.com (C. Yao), junyuanrao@qq.com (J. Rao), 1180677@qq.com (Y. Tang), 994461645@qq.com (J. Liu), 632564596@qq.com (X. Huang)*

[b]*Department of Environmental Science and Engineering, Zhongkai University of Agricultural and Engineering, Guangzhou, China, Tel. +86-020-8632-4662, email: gzzkq@126.com (H. Liu), 018646647@qq.com (H. Li)*

[c]*College of Environmental Science and Engineering, Central South University of Forestry and Technology, Changsha, China, Tel. +86-020-8632-4662, email: huxinjiang@126.com (X. Hu)*

[d]*Institute of Bast Fiber Crops, Chinese Academy of Agricultural Sciences, Changsha, China, Tel. +86-020-8632-4662, email: wanghuii623@163.com (H. Wang)*

ABSTRACT

The catalytic activity of metal nanoparticles (MNPs) relies on the property of the support. The recent availability of suspensions of graphene oxide(GO) and other graphene-based materials has provided new opportunities for the development of supported MNPs as catalysts. Herein, this work aims to develop a novel MNPs-GO catalyst possessing large surface area, strong metal–support interaction and more active sites. A magnetic nano Fe^{n+}@GO nanocomposite (MFGO) with MNPs (i.e., Fe^{n+}, iron oxide) and graphene oxide was synthesized through a facile in situ co-precipitation method. The MFGO composites were utilized as effective heterogeneous Fenton catalysts for the degradation of tetracycline (TC) over a wide pH range. The removal efficiencies for the system of H_2O_2, MFGO and H_2O_2 with MFGO after 120 min reached 19.17%, 25.38%, and 94.82%, respectively. The optimum removal efficiency achieved 94.80% in the condition of 500 mg/L TC, pH = 7.0, 0.469 mol/L H_2O_2 and 0.5 g/L catalyst dose. Besides, the catalysts could be used for at least six times. The magnetic nanoparticles had been strongly immobilized on the surface of GO through stable chemical bonding. The introduction of GO contributed to increasing the adsorption capacity and enhancing the Fenton catalytic activity. The catalysts could be magnetically recycled with good stability. This study provided new insights into the precipitation of a magnetic heterogeneous catalyst and advanced its application.

Keywords: Fe^{n+}; Graphene oxide; Tetracycline; Heterogeneous Fenton oxidation

1. Introduction

Tetracycline (TC; $C_{22}H_{24}N_2O_8$), one of the most common broad-spectrum antibiotics, is used extensively in human treatment [1], livestock husbandry and aquaculture industries [2]. Tetracycline residues are stable and usually resistant to the conventional wastewater treatments, such as, biological treatment or physical adsorption technology [3]. To overcome the drawbacks of the conventional treatments, the application of different catalytic technologies as the so-called advanced oxidation procedures (AOP's) is gaining more and more attention [4]. Recently, the Fenton technology has become one of the most powerful and widely used AOP's for the treatment of wastewater containing non-biodegrad-

*Corresponding author.

able organic pollutants [5]. For instance, Fenton systems was applied to remove tetracyclines [6]. However, there are also shortcomings of the application of the conventional Fenton method, such as (i) narrow pH range (2.8~3.2) requirement, (ii) ineffective utilization of quickly generated hydroxyl radicals ($\cdot$OH), (iii) the handling of the large amount of iron sludge after neutralization, (iv) the secondary population issue of the use of high iron concentration during mineralization. In consequence, numerous studies focused on heterogeneous Fenton-like system using metal nanoparticles (MNPs), since they have interesting properties to be potentially used as heterogeneous catalysts, such as wide availability, low cost and high specific surface area [7,8].

Among MNPs, magnetic nanoparticles are the most effectual heterogeneous Fenton catalysts and have been successfully applied for organic pollutants degradation [9,10]. In this system, magnetic nanoparticles can be decomposed by H_2O_2 molecules to produce hydroxyl radicals ($\cdot$OH) through the Fenton reaction according to Eq. (1) [11]. Magnetite or Fe_3O_4 magnetic nanoparticles significantly enhanced the formation rate of $\cdot$OH, due to the existence of octahedral sites containing Fe^{2+} ions. The produced $\cdot$OH are robust oxidant species reacting unselectively with organic compounds which results in the mineralization of these compounds into inorganic ions, CO_2 and H_2O [12]. According to Eq. (2), Fe^{2+} ions can be regenerated via the reduction of Fe^{3+} by H_2O_2.

$$Fe^{2+} + H_2O_2 \rightarrow Fe^{3+} + OH^- + {}^{\bullet}OH \tag{1}$$

$$Fe^{3+} + H_2O_2 \rightarrow Fe^{2+} + H^+ + {}^{\bullet}OOH \tag{2}$$

However, Fe_3O_4 magnetic nanoparticles have a strong tendency to agglomerate into larger ones owing to intra-particle interactions (e.g., the Van der Waals and intrinsic magnetic interactions) [13,14]. This property can decrease Fe_3O_4 magnetic nanoparticles characteristics including surface/volume ratio, dispersion stability and catalytic capability.

A useful and effective approach to overcome these problems is to incorporate magnetic nanoparticles (e.g., Fe_3O_4) into porous supporting materials viz., zeolite, activated carbon and polymer. In this method, magnetic nanoparticles are uniformly distributed on the supporter surfaces and show a high catalytic activity, compared to the single magnetic catalysts. Moreover, iron-based catalyst systems cannot only provide a high surface area for the adsorption of pollutants and oxidants, but principally improve electron transfer and subsequently the performance of oxidation process. Recently, this technique widely attracted the attention of researches because the iron immobilization onto a support provides a physical retention of the catalyst to avoid the iron release in the treated water [15].

Graphene oxide (GO), a two-dimensional (2D) nanosheet of sp^2-hybridized carbon, exhibits a high potential as a supporting material for Fenton catalysts, due to rich source of raw materials, simple preparation method, very large surface to volume ratio, high stability and wide availability [16]. Recently, some researches have focused their attentions on using reduced graphene oxide (rGO) as a catalyst for the removal of organic compounds in the Fenton oxidation studies [17]. It is reported that GO contributes on improving the performance of Fenton catalytic process

regarding the adsorption of pollutants. Therefore, there is a strong impetus to explore GO as a support material for magnetic MNPs to perform heterogeneous Fenton reaction.

In this study, a novel magnetic heterogeneous catalyst composite was synthesized by immobilizing Fe^{n+} (e.g., Fe^{2+}, Fe^{3+}) to graphene oxide (MFGO). The catalytic activity was estimated by the degradation of Tetracycline (TC). The objectives of this work are (1) to prepare and characterize a magnetic nano Fe^{n+}@GO (MFGO) and apply it as a heterogeneous catalyst for the removal of TC residuals from aqueous solutions in a batch system; (2) to optimize the removal conditions by investigating the effects of solution pH, initial H_2O_2 concentration, catalyst dosage and initial concentration of TC; (3) to examine the degradation mechanisms between TC and MFGO based on the structure, morphology and property; and (4) to assess the reusability performance of MFGO.

2. Experimental

2.1. Materials

Tetracycline hydrochloride ($C_{22}H_{24}N_2O_8 \cdot HCl$, molecular weight (MW): 480.9 g/mol) was obtained from Aladdin Reagent Co., Ltd. (Shanghai, China). Graphite powder (particle size ≤30 µm) was purchased from Tianjin Fuchen Chemical Reagent Factory. Nitric acid (HNO_3), sulfuric acid (H_2SO_4, 95–98%), ethanol, sodium hydroxide (NaOH), ferric chloride hexa-hydrated ($FeCl_3 \cdot 6H_2O$), ferrous sulfate hepta-hydrate ($FeSO_4 \cdot 7H_2O$), hydrogen peroxide (H_2O_2, 30%) and some other chemicals used in the experiments were of analytical-laboratory grade and supplied by Sinopharm Chemical Reagent Co., Ltd (Shanghai, China). Only high-purity water (18.25 MΩ/cm) purified through a Millipore system was used in all experiments.

2.2. Synthesis of catalyst

Graphene oxide (GO) was synthesized from natural flake graphite powder according to the modified Hummers protocol [18–20]. Briefly, the natural graphite powder was first pre-oxidized with $K_2S_2O_8$, P_2O_5 and H_2SO_4, then further oxidized with H_2SO_4, $NaNO_3$ and $KMnO_4$. Lastly, the resulting mixture was rinsed repeatedly with Milli-Q water and then sonicated to obtain a GO suspension.

The catalyst was prepared by a facile in situ chemical co-precipitation method. In brief, 14 g $FeCl_3 \cdot 6H_2O$ and 5 g $FeSO_4 \cdot 7H_2O$ were dissolved in 200 mL of Milli-Q water. The Fe^{2+} and Fe^{3+} solution was added into 500 mL of GO suspension under vigorous stirring at 450 rpm for 2 min in water-bath thermometer. Then, NaOH solution (100 g/L) was added rapidly to adjust the solution pH to 10–11, and the mixture was stirred continuously at 258 K for 45 min to form magnetic nano Fe^{n+}@GO composite. After cooling at room temperature, the product was separated from the suspension using a magnet and washed with Milli-Q water several times until the solution pH became neutral.

The magnetic nano Fe^{n+}@GO was defined simply as MFGO. And the products were employed as heterogeneous Fenton catalysts in the experiment at a concentration of 15±0.10 mg/mL.

2.3. Characterization methods

The morphology and structure were analyzed by scanning electron microscopy (SEM; Hitachi, S-4800, Japan) and high-resolution transmission electron microscopy (HRTEM; Tecnai G2-F20, USA). Energy dispersive spectrometry (EDS) mapping was conducted using the EDAX system attached to the same field-emission transmission electron microscope. TG and DSC curves were measured by thermoanalytical equipment (TGA; SDT Q600, USA) under a nitrogen atmosphere from room temperature to 1273 K. Fourier transform-infrared spectroscopy (FT-IR) spectra of the samples were measured in wave numbers ranging from 400 to 4000 cm^{-1} using a Perkin-Elmer Spectrum One spectrometer (Magna-IR 170, Nicolet, Ltd., USA) with a KBr beam splitter at room temperature. The surface elemental composition was recorded on X-ray photoelectron spectroscopy (XPS; Thermo ESCALAB 250Xi, USA) with a resolution of 0.5 eV. The vibrating sample magnetometer (VSM; MPMS-XL-7, Quantum Design Instruments, USA) was used to assess the magnetization measurement curve at room temperature.

2.4. Removal experiments

A stock solution (10 g/L) of TC was prepared by dissolving specific amounts of TC powder into Milli-Q water. The different concentrations of TC solutions used in the batch experiments were obtained by diluting the stock solution. Experiments regarding the degradation processes of TC by heterogeneous Fenton system (MFGO/H$_2$O$_2$) were conducted in conical flasks containing 150 mL of the prepared solutions of TC with a temperature-controlled shaker (298 K) at a constant speed of 160 rpm. Firstly, a certain amount of catalyst was added into TC solution and the suspension was stirred in the dark overnight to achieve an adsorption/desorption equilibrium. Then, the H$_2$O$_2$ solution was added into the sample solution to initiate the Fenton reaction. At selected time intervals, the catalyst was magnetically separated from the solution by a magnet. The filtered sample (0.45 μm) was analyzed by an ultraviolet and visible spectrophotometer (UV-1780) to obtain the residual TC concentration. The maximum wavelength of TC was determined at 357 nm. The removal efficiency of TC is calculated according to Eq. (3). In this study, the pH was adjusted to the desired value via adding negligible volumes of NaOH or HNO$_3$. And the effects of variables such as pH, catalyst and H$_2$O$_2$ concentration, as well as the initial TC concentration on the removal efficiency were investigated. After process optimization, the reusability, stability and mineralization of the catalyst were evaluated in six consecutive cycles of use.

$$\text{Removal Efficiency} = (C_0 - C)/C_0 \times 100\% \tag{3}$$

where C_0 (mg/L) and C (mg/L) were the initial and remnant concentration of TC, respectively.

3. Results and discussion

3.1. Characterization

The SEM image of the sample is shown in Fig. 1a. The image revealed that there were many intrinsic wrinkles on the external surface of MFGO, which were essential for the structural stability of MFGO. This could also be attributed to the agglomeration and uniform distribution of the active species (i.e., Fe^{n+}, iron oxide) on the GO surface, which increased its adsorption capability for pollutant adsorption. The TEM image of MFGO (Fig. 1b) depicted a typical fabric-like shape with a two-dimensional nanosheet structure. As can be seen, numerous nanoparticles loaded on GO nanosheets. Similar results had been reported previously [20], the external surface of the MFGO composite was rough and irregular due to the loading of the nanoparticles, demonstrating the potential application of the synthesized composite on pollutant degradation.

The EDS spectrum (Fig. 1c) indicated that carbon (C), oxygen (O) and iron (Fe) were present in the structure of MFGO. However, the C was mainly contained in the GO sheets, while the O was present in the iron oxide and the oxygen-containing functional groups of GO [21].

The surface functionalities of MFGO were identified from the FT-IR spectra, as shown in Fig. 2a. The peak at 3408 cm^{-1} corresponded to hydrogen-bonded (–OH) stretching vibrations [22]. The peak at 1629 cm^{-1} was ascribed to aromatic C=C groups [23]. The peaks at 1428 cm^{-1} and 1005 cm^{-1} could be respectively attributed to epoxy C-O and alkoxy C-O stretching vibrations in COH/COC of the MFGO [24]. Besides, the absorption peak located at 538 cm^{-1} corresponded to the Fe-O stretching vibration of iron oxide; this was owing to the successful connections between the magnetic nanoparticles and the GO nanosheets, which was
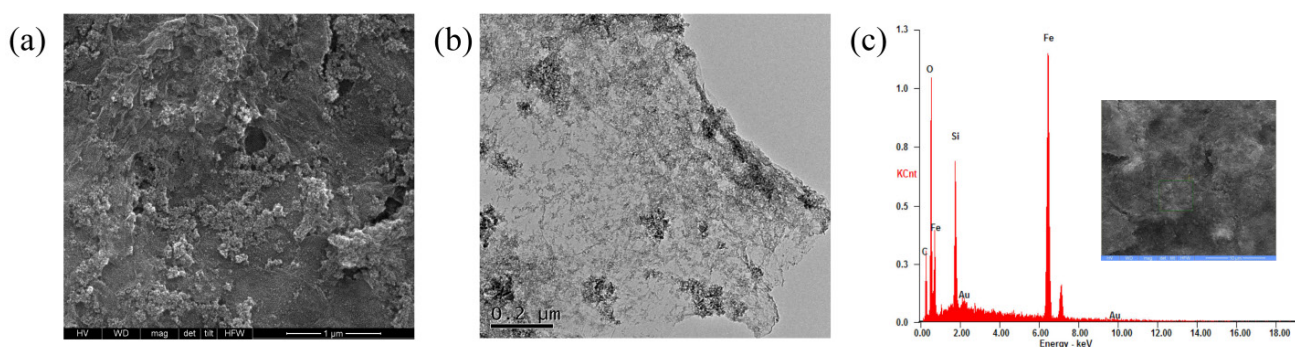
Fig. 1. (a) SEM image, (b) HRTEM image and (c) EDS image of MFGO.

consistent with previous literature [25]. This result also indicated that the active species (i.e., Fe^{n+}, iron oxide) were immobilized on the surface of graphene oxide with a stable bonding.

The TG-DSC curves of MFGO showed several decomposition steps in Fig. 2b. The first step with 7.29 wt.% loss of mass between 297 K and 359 K was attributed to the evaporation of adsorbed water molecules [26]. Then, the rate of weight loss between 359 K and 900 K was relatively high, which indicated that low molecular weight compounds and magnetic nanoparticles were decomposed [27]. In the third stage, the distinct weight loss of 23.61% appeared at 900 K-955 K, which was ascribed to the bulk pyrolysis of carbon skeletons and the oxygen-containing functional groups such as carboxyl, epoxide and hydroxyl from the MFGO sheets [28]. The slight weight loss (2.54%) occurred from 955 K to 1273 K was due to the carbon remnants from MFGO composite [29].

The information on the elemental composition and chemical status of the composite (MFGO) were obtained in XPS analysis; the results were shown in Figs. 2c–2e. From the full survey scan of XPS spectra (Fig. 2c), three distinct peaks corresponding to C 1s, O 1s and Fe 2p were obtained. The C 1s spectrum of MFGO (Fig. 2d) was fitted into five peaks at 284.7, 284.9, 285.6, 286.6 and 288.3 eV, attributing to C-C/C=C, C-O, C-O-C, C=O and O-C=O groups, respectively [30]. The Fe 2p XPS spectra of MFGO is shown in Fig. 2e. The peaks at 710.8 and 724.3 eV were correlated to Fe^{2+} while the peaks at 712.3 and 726.0 eV were correlated to Fe^{3+} on the MFGO surface [31]. The atomic percentages of C, O and Fe were obtained from XPS characterization analysis. And the atomic ratio of C, O and

Fe was about 53.68:37.42:8.9. These results indicated that the surfaces of GO might be loaded by nanoparticles (i.e., Fe^{n+}, iron oxide) [32].

Fig. 2f illustrates the magnetic hysteresis loop of MFGO at room temperature in a magnetic field of ±20 kOe. As it was noted, the saturation magnetization (Ms) of MFGO was 9.53 emu/g. The remnant magnetization (Mr) was 0.15 emu/g and the coercive force (Hc) was 18.53 Oe (bottom right of Fig. 2f), which indicated rather little residual magnetization when the additive magnetic field was removed and MFGO showed a super paramagnetic property [33]. Moreover, MFGO could be easily separated from solution by an external magnetic field in a short time and be potentially used as a recoverable magnetic catalyst to remove contaminants from aqueous environment to prevent the secondary pollution (top left of Fig. 2f).

3.2. Removal of tetracycline under different systems

Fig. 3 demonstrates the performance of H_2O_2 alone, MFGO alone and MFGO with H_2O_2 on the removal of 500 mg/L of TC under the condition of pH = 7.0, H_2O_2 dosage of 0.469 mol/L, and the catalyst dosage of 0.5 g/L during 300 min of reaction. It was found that a low removal efficiency of 19.17% was obtained from with H_2O_2 after 120 min reaction, which indicated that TC could hardly be degraded with only H_2O_2 due to the weak oxidation ability of H_2O_2. The removal efficiency obtained with MFGO was 25.38%, higher than that of H_2O_2 alone, which was mainly owing to the surface adsorption [34]. It demonstrated that the direct oxidation of TC by H_2O_2 and its adsorption by MFGO were limited.
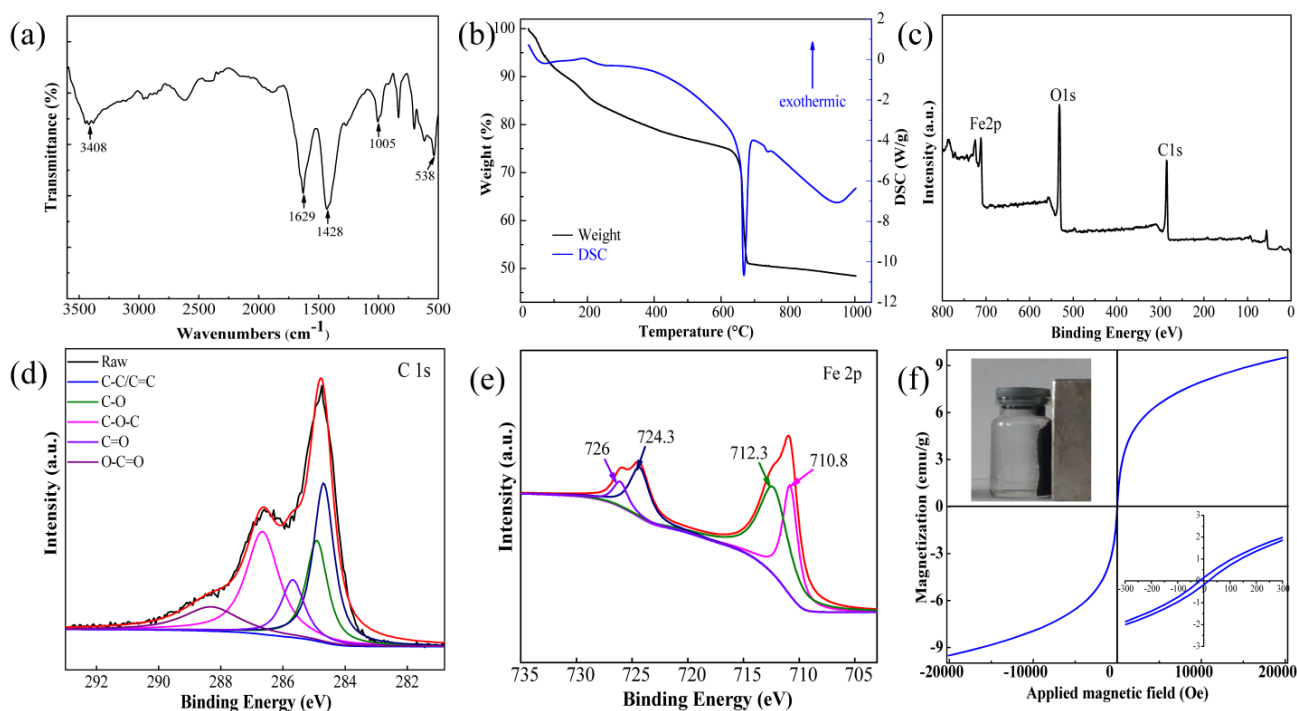
Fig. 2. (a) FT-IR spectra; (b) TG-DSC spectra; (c) Full survey scan of XPS spectra of MFGO; XPS spectra of (d) C1s, (e) Fe2p of MFGO; (f) Magnetization loop of MFGO (The top inset displayed MFGO composites dispersion and magnetic separation. The bottom insert illustration was a partial enlarged view near its origin.)

As exhibited in Fig. 3, the removal efficiency of TC for MFGO with H_2O_2 system was noticeably enhanced at the beginning of the reaction and then reached the equilibrium (94.82%) at 120 min, which was significantly greater than the removal efficiencies of MFGO or H_2O_2 each alone. This high performance might be explained by the fact that both processes (i.e., adsorption and Fenton oxidation) were involved in the removal of TC simultaneously [8,35]. Firstly, the synergistic effect between the active species (i.e., Fe^{n+}, iron oxide) and GO was contributed to the availability of additional adsorption sites to TC, which could result in an increase on the degradation of TC by MFGO [36]. Secondly, the heterogeneous catalytic reaction played an important role in the removal of TC. Furthermore, the surface hydroxyl radicals were identified as the major reactive species during the heterogeneous Fenton processes [11]. In these processes, as described in Eqs. (1) and (2), the couple of Fe^{2+}/Fe^{3+}, as a catalyst, could catalyze H_2O_2 to produce $^\bullet OH$ and $^\bullet OOH$ [12].

In addition, the H_2O_2 activating ability and the catalytic activity were both improved through uniform distribution of magnetic nanoparticles (i.e., Fe^{n+}, iron oxide) on the GO surface, which also avoided the agglomeration of magnetic nanoparticles. Therefore, the synergistic effects of Fe^{n+}, iron oxide nanoparticles, graphene oxide and H_2O_2 all contributed to the high efficient removal of TC.

3.3. Effects of solution pH

The pH value of the solution was an important factor affecting the Fenton oxidation of organic contaminates. In this study, the effect of initial pH value of solutions on the removal of TC in MFGO/H_2O_2 system was examined at various pH values (i.e., 3, 5, 7, 9 and 11). The adsorption was the first step for developing the heterogeneous Fenton catalyst. As shown in Fig. 4, the adsorption experiments suggested that less than 44.37% of TC was removed without the help of H_2O_2. In the heterogeneous catalytic reaction, the TC removal efficiency declined as the pH values increased from 3.0 to 11.0. After 120 min of reaction time, 96.30% of TC
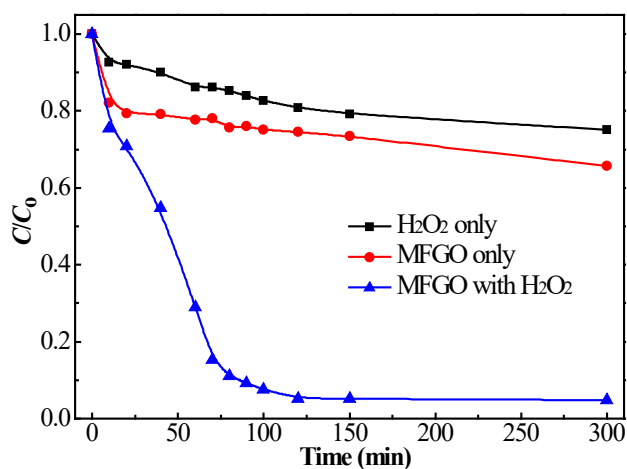
was removed when the pH of solution was set at 3.0, while 88.19% degradation was achieved when the pH was 11.0. This is because MFGO was easily dissolved at lower pH, and more Fe^{2+} ions were released, resulting in more $^\bullet OH$ generation [37]. However, as pH increased, the generation of $^\bullet OH$ was reduced due to the formation of Fe^{2+} complexes (e.g., FeO^{2+}) (Eq. (4)), as well as the deactivation of catalyst with the formation of ferric hydroxide complex, and subsequently, the activation rate of H_2O_2 and $^\bullet OH$ production decreased [38]. Moreover, a related literature reported that Fe^{3+} oxyhydroxides (e.g., $FeOH^{2+}$, $Fe(OH)^{2+}$, $Fe_2(OH)_2^{4+}$, $Fe(OH)_3^o$, and $Fe(OH)_4^-$) presented low activation efficiencies for H_2O_2 to produce $^\bullet OH$ [39].

$$Fe^{2+} + H_2O_2 \rightarrow FeO^{2+} + H_2O \tag{4}$$

According to Fig. 4, the removal efficiency of TC at pH 7.0 within 120 min was larger than 90%. This phenomenon might be because that the Fe^{2+} ions on the catalyst could induce the production of adsorbed $^\bullet OH$ at neutral pH value [40]. Besides, the Fe^{3+} produced during the reaction was immobilized on the catalyst. Therefore, the active species (i.e., Fe^{n+}, iron oxide) on the catalyst surface would maintain its catalytic activity to produce $^\bullet OH$ at neutral pH [41]. In this case, the tetracycline could be removed completely under neutral conditions if the reaction time was enough. This finding indicated that MFGO performed well in a wide pH range. Taking all of the above-mentioned into consideration, pH = 7.0 was selected for the removal of TC in MFGO/H_2O_2 system.

3.4. Effects of H_2O_2 concentration

In a Fenton oxidation system, the oxidant concentration is a major factor which significantly influences the degradation of organic substrates [42]. The effect of H_2O_2 concentration on TC removal experiment was conducted in the range of 0.2–1.5 mol/L H_2O_2 under a fixed MFGO dose (0.5 g/L), pH 7.0 and 500 mg/L TC. As shown in Fig. 5, the adsorption experiments showed that 41.08% of TC was removed in the

Fig. 3. TC removal efficiency under different conditions. Reaction condition: m/V = 0.5 g/L, $C_{0(TC)}$ = 500 mg/L, H_2O_2 = 0.469 mol/L, T = 298 K, pH = 7.0.
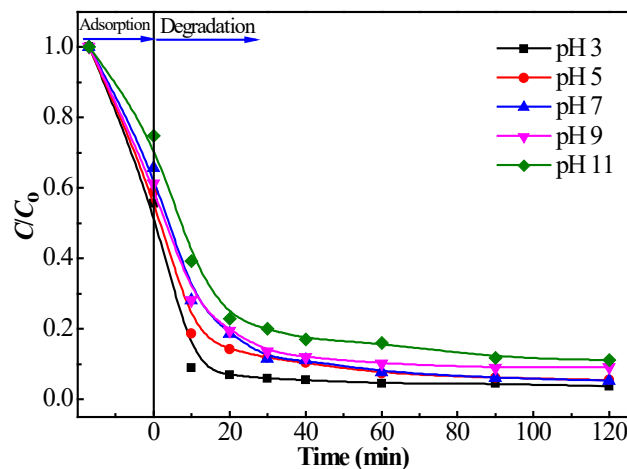
Fig. 4. Effect of solution pH on TC removal by MFGO/H_2O_2 system. Reaction condition: m/V = 0.5 g/L, H_2O_2 = 0.469 mol/L, $C_{0(TC)}$ = 500 mg/L, T = 298 K.
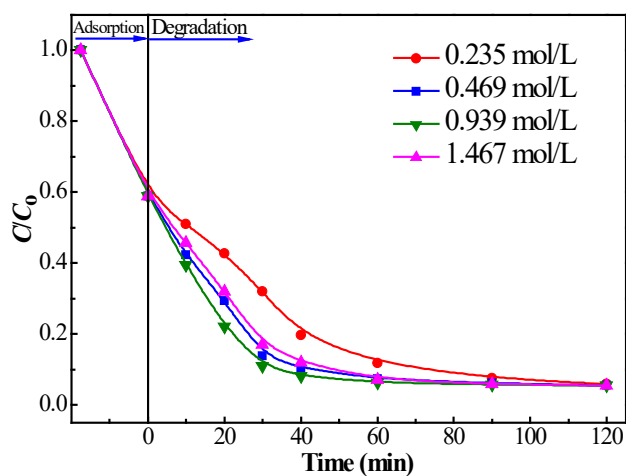
Fig. 5. Effect of initial H_2O_2 concentration on TC removal by MFGO/H_2O_2 system. Reaction condition: m/V = 0.5 g/L, $C_{0(TC)}$ = 500 mg/L, pH = 7.0, T = 298 K.

Fig. 6. Effect of catalyst dose on TC removal by MFGO/H_2O_2 system. Reaction condition: $C_{0(TC)}$ = 500 mg/L, H_2O_2 = 0.469 mol/L, pH = 7.0, T = 298 K.

absence of H_2O_2. 94.53% and 94.56% of TC removal efficiency after 120-min oxidation reaction were achieved for 0.469 and 0.939 mol/L H_2O_2, respectively. However, the TC removal efficiency (94.57%) hardly enhanced when the H_2O_2 concentration further increased to 1.467 mol/L. This phenomenon might be explained that more H_2O_2 molecules could reach the surface of MFGO and subsequently reacted with Fe^{n+} to generate more reactive radicals with the increasing of H_2O_2 concentration within a certain H_2O_2 concentration range [43]. However, excessive addition of H_2O_2 could not further improve the removal efficiency, which could be attributed to the scavenging effect of $\cdot OH$. Moreover, the excessive H_2O_2 acted as a scavenger of the highly potential hydroxyl radicals [Eq. (5)], generating perhydroxyl radicals [44].

$$\cdot OH + H_2O_2 \rightarrow \cdot OOH / \cdot OO^- + H_2O \tag{5}$$
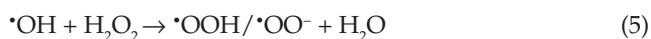
Additionally, $\cdot OH$ was consumed, and instead, $\cdot OOH$ was generated. $\cdot OOH$ was much less reactive than $\cdot OH$, which led to the reduction of the TC removal efficiency [45]. Hence, the optimum H_2O_2 concentration for the removal of TC in the this study was 0.469 mol/L.

3.5. Effects of catalyst dosage

The catalyst dosage directly affects the generation of active radicals. Fig. 6 shows that various dosages of MFGO impacting MFGO on the removal of TC, where H_2O_2 concentration was 0.469 mol/L at initial pH 7.0 and initial TC concentration of 500 mg/L. During the adsorption phase, it's observed that the amount of TC adsorbed on the catalyst surface increased as the amount of MFGO catalyst increased. In the oxidation process, the degradation efficiencies were 90.95%, 94.53%, 94.20%, and 95.44% after 120-min degradation when the MFGO was 0.2, 0.5, 0.7 and 0.9 g/L, respectively. Therefore, the degradation efficiency increased when the MFGO dosage increased from 0.2 to 0.5 g/L. This was because the rise in the catalyst concentration favored the release of more active sites (i.e., Fe^{n+}, iron oxide)
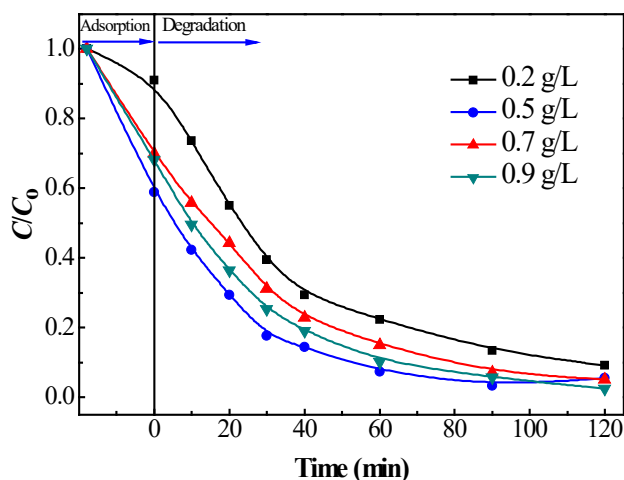
into solution, and consequently it could also accelerate the decomposition of H_2O_2 to $\cdot OH$ [46]. However, the degradation efficiency didn't show a further increase when the catalyst dosage exceeded 0.5 g/L, which was ascribed to the scavenging effect of hydroxyl radicals through the undesirable reaction (Eq. (6)) [47].

$$Fe^{2+} + \cdot OH \rightarrow Fe^{3+} + OH^- \tag{6}$$

Several authors [48] also indicated that at higher concentrations of Fe^{2+} or Fe_3O_4, as the activators of H_2O_2, the ultimate oxidizing power was limited by the destruction of $\cdot OH$ radicals in the presence of excessive Fe^{2+} or the rapid conversion of all Fe^{2+} to Fe^{3+}.

3.6. Effects of initial TC concentration

The initial concentration of TC solution was another important parameter in Fenton reaction. As shown in Fig. 7, the effect of initial TC concentration on TC degradation was investigated in the range of 100–750 mg/L TC. Within 120 min, the removal percentages were 99.90%, 98.31%, 94.53% and 90.97% for TC solutions with the initial concentrations of 100, 250, 500 and 750 mg/L, respectively. The removal percentage significantly declined as the initial TC concentration increased. This is because more and more TC molecules were adsorbed on MFGO surface and occupied a larger number of active sites (i.e., Fe^{n+}, iron oxide), which became unavailable for H_2O_2 and resulted in less $\cdot OH$ generation [49]. Higher TC concentration also inhibited the reaction of H_2O_2 at the redox-active centers. Besides, fixed concentrations of catalyst and H_2O_2 against the increase in the initial TC concentrations present lower removal efficiencies for TC by MFGO/H_2O_2 system. The same results was described in previous studies [48,49]. In addition, when the initial TC concentration was low, the $\cdot OH$ production rate would be higher than the consumption rate leading to a higher TC removal efficiency. Thus, the initial concentration of TC was set to 500 mg/L in further experiments.
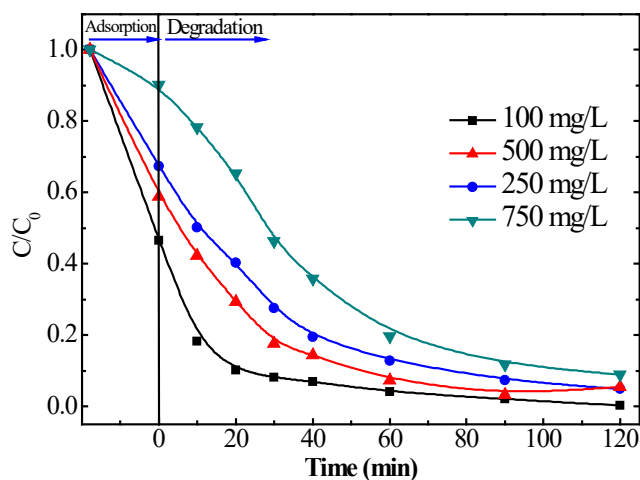
Fig. 7. Effect of catalyst dose on TC removal by MFGO/H$_2$O$_2$ system. Reaction condition: $m/V = 0.5$ g/L, $C_{0(TC)} = 100$, 250, 500, 700 mg/L, H$_2$O$_2 = 0.469$ mol/L, pH = 7.0, $T = 298$ K.

3.7. Kinetic analysis

The heterogeneous Fenton process can be described by a pseudo-first-order kinetic model [50]. In this study, we evaluated the kinetics of TC degradation using pseudo-first-order model. Fig. 8 depicts the pseudo-first-order plots of TC removal by MFGO/H$_2$O$_2$ system with different TC, catalyst and H$_2$O$_2$ concentration. The corresponding pseudo-first-order model fitting constants (i.e., K) are summarized in the inset table in Figs. 8a–c.

The model presents a high regression coefficient ($R^2 > 0.94$) for all studied parameters (i.e., TC and catalyst concentrations). This confirms that the pseudo-first-order model was a great fit to describe the degradation behavior of TC in MFGO/H$_2$O$_2$ system. Fig. 8 displays the coherence between the experimental data from the studied process and those from the kinetic reaction model with different concentrations of TC and catalyst. The degradation rate was inversely proportional to the initial TC concentration, as shown in Fig. 8a. According to the results presented in the inset table in Fig. 8a, the values of the reaction rate constant, K, decreased from 0.03567 to 0.02084 min^{-1} as the initial TC concentration increased from 100 to 750 mg/L. Moreover, lower concentration of TC offered faster degradation rate compared to the higher concentrations, which was because the amounts of catalyst and H$_2$O$_2$ were relatively limited when the TC concentration was high. In a further related development, , the largest K occurred when the MFGO concentration increased to 0.5 g/L (Fig. 8b). And an excess of catalyst caused a decrease in the reaction rate. Therefore, the following experiments were carried out using a catalyst concentration of 0.5 g/L. Moreover, Fig. 8c shows that the reaction rate constants increased along with the rise in H$_2$O$_2$ concentration, with the corresponding values of 0.02829, 0.03163, 0.02878 and 0.02694 min^{-1} with the H$_2$O$_2$ concentration of 0.235, 0.469, 0.939 and 1.467 mol/L, respectively (see Fig. 8c). The best obtained degradation performance appeared when using 0.469 mol/L of H$_2$O$_2$.

TC con. (mg/L)	K (1/min)	R^2
100	0.03567	0.94025
250	0.02221	0.97074
500	0.03163	0.99449
750	0.02084	0.96577

(a)

Catalyst con. (g/L)	K (1/min)	R^2
0.2	0.01934	0.96675
0.5	0.03163	0.99449
0.7	0.02271	0.97922
0.9	0.02713	0.99128

(b)

H2O2 con. (mol/L)	K (1/min)	R^2
0.235	0.02829	0.96568
0.469	0.03163	0.99449
0.939	0.02878	0.82656
1.467	0.02694	0.93203
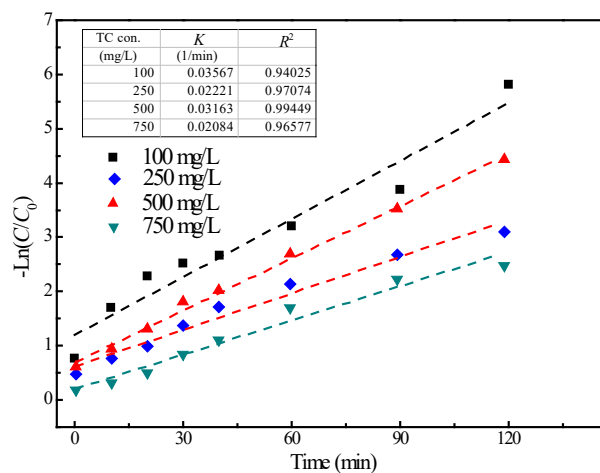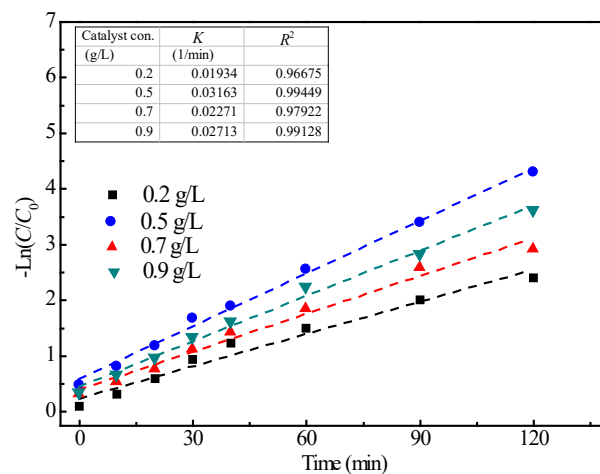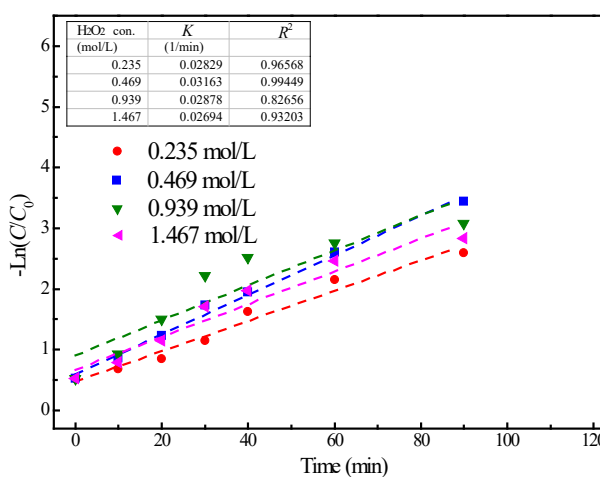
(c)

Fig. 8. Effect of various TC (a), MFGO (b) and H$_2$O$_2$ (c) concentrations on the pseudo-first-order rate of TC degradation by MFGO/H$_2$O$_2$ system and the values of degradation kinetics constants of TC by MFGO/H$_2$O$_2$ system (inset).

3.8. Reusability of the catalyst

The reusability of the catalyst, from the practical point of view, is an important property [51]. The reusability of MFGO was tested for six consecutive runs under the optimum reaction conditions (0.469 mol/L H_2O_2, 500 mg/L TC, 0.5 g/L catalyst and pH 7.0) for a period 120 min. In each cycle of use, the catalyst was separated from the reaction solution using a magnet and then applied for the next experiment. As shown in Fig. 9, the TC removal efficiencies for six cycles of MFGO/H_2O_2 system were 93.71%, 93.15%, 92.10%, 91.29%, 87.94% and 86.37%, respectively. In this process the ability of TC removal was only slightly declined, indicating that MFGO showed an excellent reusability without significant loss in catalytic activity.

However, there was a non-negligible drop in the TC degradation efficiency (7.3%), and the decrease of catalytic activity might be due to two reasons: firstly, the surface of the catalyst was partly covered by TC reactants and the residual by-products [52]; secondly, iron oxide surface on leaching might cause the loss of the catalyst activity [53]. Even though the activity of the catalyst dropped in some extent, the catalyst still displayed the reusability for the practical use for its convenient magnetic separation advantage. Therefore, MFGO can potentially be applied as a reusable catalyst to remove TC or other antibiotics.

In addition, we proposed a possible mechanism of the Fenton reaction catalyzed by MFGO. The reaction starts with the formation of a precursory surface complex by H_2O_2 and Fe^{3+}. Then the complex decomposes to Fe^{2+} and $\cdot OH$ by a reversible electron transfer, triggering a series of chain reaction involving the formation of $\cdot OH$ and the redox cycle of Fe^{3+}/Fe^{2+} [54]. In fact, this step is the rate-limiting step of the whole heterogeneous catalytic reaction, as its rate constants is much lower than other steps [55]. Nevertheless, it is facilitated with the Fe^{n+} complex and further the π-π stacking with GO, thus creates an excellent catalytic ability of MFGO. At the same time, hydroxyl radicals mainly attack organics adsorbed on the near-surface of the catalyst, avoiding the effect of HO^- and other possible scavengers from the bulk solution.
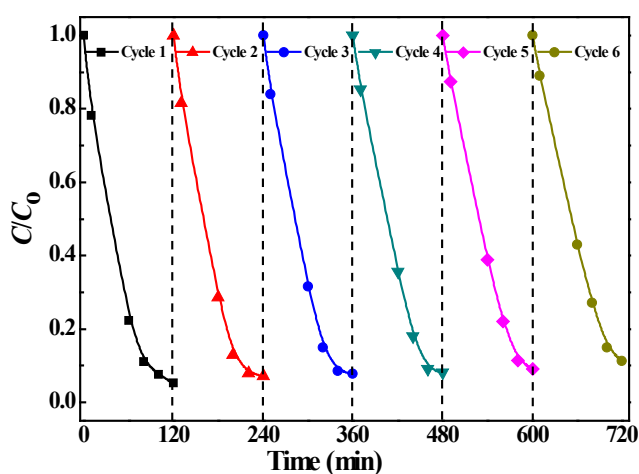
Fig. 9. Reusability of TC in 6 successive cycles. Reaction condition: m/V = 0.5 g/L, $C_{0(TC)}$ = 500 mg/L, H_2O_2 = 0.469 mol/L, pH = 7.0, T = 298 K.

4. Conclusions

In this work, a simple and green method based on the previously reported studies [18–20] was applied on the preparation of magnetic nano $Fe^{n+}@GO$ composite (MFGO), which was the key technology to obtain the in situ growth of magnetic nanoparticles (i.e., Fe^{n+}, iron oxide) on the GO sheets without the help of any additional reducing agents and organic surfactants. The characterization studies revealed that more surface-active reactive species were generated on MFGO surface attributing to the special support structure. Iron existed in a multivalent state, which was beneficial for enhancing MFGO Fenton activity [32]. Compared with similar Fe-based catalysts (e.g., Fe-based MOFs, $Fe_3O_4/rGO/TiO_2$) [8,35], MFGO exhibited much better removal efficiency towards TC benefiting from the synergistic effect of adsorption and heterogeneous Fenton reaction. Under the optimum condition (0.469 mol/L of H_2O_2, 0.5 g/L of catalyst, pH 7.0), 94.80% degradation of TC (500 mg/L) was realized within 120 min. This demonstrated that TC could be degraded at room temperature in MFGO/H_2O_2 system. This further indicated that $\cdot OH$ radicals played a primary role in the catalytic oxidation pathway as described previously by other researchers [37–39,49]. Importantly, MFGO exhibited high catalytic activity over a wider pH range of 3.0–11.0 without any external energy input. Furthermore, MFGO showed no obvious loss of catalytic activity even after 6 successive runs, which indicated a high reusability and a good structural stability in comparison with related magnetic materials [52,53]. High reaction activation, potential magnetic reusability, together with a simple precipitation process, made MFGO a promising reusable catalyst in the practical treatments of TC or other antibiotics.

References

[1] Y. Chen, K. Liu, Preparation and characterization of nitrogen-doped TiO_2/diatomite integrated photocatalytic pellet for the adsorption-degradation of tetracycline hydrochloride using visible light, Chem. Eng. J., 302 (2016) 682–696.

[2] H. Zhao, X. Liu, Z. Cao, Adsorption behavior and mechanism of chloramphenicols, sulfonamides, and non-antibiotic pharmaceuticals on multi-walled carbon nanotubes, J. Hazard. Mater., 310 (2016) 235.

[3] C.Q. Chen, J. Li, P.P. Chen, R. Ding, P.F. Zhang, X.Q. Li, Occurrence of antibiotics and antibiotic resistances in soils from wastewater irrigation areas in Beijing and Tianjin, China, Environ. Pollut., 193 (2014) 94–101.

[4] Y. Chen, N. Li, Y. Zhang, Novel low-cost Fenton-like layered Fe-titanate catalyst: preparation, characterization and application for degradation of organic colorants, J. Colloid Interf. Sci., 422 (2014) 9–15.

[5] R. Huang, Z. Fang, X. Fang, E.P. Tsang, Ultrasonic Fenton-like catalytic degradation of bisphenol a by ferroferric oxide (Fe_2O_4) nanoparticles prepared from steel pickling waste liquor, J. Colloid Interf. Sci., 436 (2014) 258–266.

[6] Y. Ghaffari, A. Mahvi, M. Alimohammadi, Evaluation of Fenton process efficiency in removal of tetracycline from synthetic wastewater, Mazandaran Univ. Med. Sci., 27 (2017) 291–305.

[7] R. Li, X. Jin, M. Megharaj, R. Naidu, Z. Chen, Heterogeneous Fenton oxidation of 2,4-dichlorophenol using iron-based nanoparticles and persulfate system, Chem. Eng. J., 264 (2015) 587.

[8] D.B. Wang, F.Y. Jia, H. Wang, F. Chen, Y. Fang, W.B. Dong, G.M. Zeng, Efficient adsorption and photocatalytic degradation of tetracycline by Fe-based MOFs, J. Colloid Interf. Sci., 519 (2018) 273–284.

[9] L. Liu, G. Zhang, L. Wang, T. Huang, L. Qin, Highly active S-modified $ZnFe_2O_4$ heterogeneous catalyst and its photo-Fenton behavior under UV À visible irradiation, Ind. Eng. Chem. Res., 50 (2011) 7219–7227.

[10] L. Truong-Phuoc, C. Pham-Huu, V. Da Costa, I. Janowska, Few-layered graphene-supported palladium as a highly efficient catalyst in oxygen reduction reaction, Chem. Commun., 50 (2014) 14433–14435.

[11] R. Molina, F. Martinez, J.A. Melero, D.H. Bremner, A.G. Chakinala, Mineralization of phenol by a heterogeneous ultrasound/fe-sba-15/H_2O_2, process: multivariate study by factorial design of experiments, Appl. Catal. B: Environ., 66 (2006) 198–207.

[12] A.J. Jafaria, B. Kakavandi, N. Jaafarzadeh, R.R. Kalantary, M. Ahmadi, Heterogeneous Fenton-like catalytic oxidation of tetracycline by AC@Fe_3O_4, as a heterogeneous persulfate activator: Adsorption and degradation studies, J. Ind. Eng. Chem., 45 (2017) 323–333.

[13] B. Kakavandi, A. Takdastan, N. Jaafarzadeh, M. Azizi, A. Mirzaei, A. Azari, Application of Fe_3O_4@C catalyzing heterogeneous UV-Fenton system for tetracycline removal with a focus on optimization by a response surface method, J. Photochem. Photobiol. A: Chem., 314 (2016) 178–188.

[14] A.A. Babaei, A. Azari, R.R. Kalantary, B. Kakavandi, Enhanced removal of nitrate from water using nZVI@MWCNTs composite: synthesis, kinetics and mechanism of reduction, Water Sci. Technol., 72 (2015) 1988–1999.

[15] M. Liu, C. Chen, J. Hu, X. Wu, X. Wang, X. Wu, X. Wang, Synthesis of magnetite/graphene oxide composite and application for cobalt(ii) removal, J. Phys. Chem. C, 115 (2011) 25234–25240.

[16] P. Zhang, J.L. Gong, G.M. Zeng, C.H. Deng, H.C. Yang, H.Y. Liu, Cross-linking to prepare composite graphene oxide-framework membranes with high-flux for dyes and heavy metal ions removal, Chem. Eng. J., 322 (2017) 657–666.

[17] S.Q. Liu, B. Xiao, L.R. Feng, S.S. Zhou, Z.G. Chen, C.B. Liu, Graphene oxide enhances the Fenton-like photocatalytic activity of nickel ferrite for degradation of dyes under visible light irradiation, Carbon, 64 (2013) 197–206.

[18] W.S. Hummers, R.E. Offeman, Functionalized graphene and graphene oxide: materials synthesis and electronic applications, J. Am. Chem. Soc., 80 (1958) 1339.

[19] D.A. Dikin, S. Stankovich, E.J. Zimney, R.D. Piner, G.H. Dommett, G. Evmenenko, Preparation and characterization of graphene oxide paper, Nature, 448 (2016) 457–460.

[20] Y. Yang, X. Hu, Y. Zhao, Decontamination of tetracycline by thiourea-dioxide-reduced magnetic graphene oxide: effects of ph, ionic strength, and humic acid concentration, J. Colloid Interf. Sci., 495 (2017) 68–77.

[21] X.J. Hu, Y.G. Liu, H. Wang, Removal of Cu(ii) ions from aqueous solution using sulfonated magnetic graphene oxide composite, Sep. Purif. Technol., 108 (2013) 189–195.

[22] H.W. Wang, Z.A. Hu, Y.Q. Chang, Y.L. Chen, Z.Y. Zhang, Y.Y. Yang, H.Y. Wu, Preparation of reduced graphene oxide/cobalt oxide composites and their enhanced capacitive behaviors by homogeneous incorporation of reduced graphene oxide sheets in cobalt oxide matrix, Mater. Chem. Phys., 130 (2011) 672–679.

[23] R.S. Dey, S. Hajra, R.K. Sahu, A rapid room temperature chemical route for the synthesis of graphene: metal-mediated reduction of graphene oxide, Chem. Commun., 48 (2012) 1787–1789.

[24] W. Wang, K. Xiao, L. Zhu, Long-term prognostic implications and therapeutic target role of hexokinase II in patients with nasopharyngeal carcinoma, Rsc Adv., 7 (2016) 21287–21297.

[25] E. Doustkhah, S. Rostamnia, Covalently bonded sulfonic acid magnetic graphene oxide: Fe_3O_4@GO-Pr-SO_3H as a powerful hybrid catalyst for synthesis of indazolo phthalazine triones, J. Colloid Interf. Sci., 478 (2016) 280–287.

[26] M. Rathod, S. Haldar, S. Basha, Nanocrystalline cellulose for removal of tetracycline hydrochloride from water via biosorption: equilibrium, kinetic and thermodynamic studies, Ecol. Eng., 84 (2015) 240–249.

[27] L. Ludueña, D. Fasce, V.A. Alvarez, Nanocellulose from rice husk following alkaline treatment to remove silica, Bioresources, 6 (2011) 1440–1453.

[28] Y. Yang, J. Wang, J. Zhang, Exfoliated graphite oxide decorated by pdmaema chains and polymer particles, Langmuir Acs J. Surf. Colloids, 25 (2009) 11808–11814.

[29] J.G. Hiremath, N.S. Khamar, S.G. Palavalli, Paclitaxel loaded carrier based biodegradable polymeric implants: preparation and in vitro, characterization, Saudi Pharm. J., 21 (2013) 85–91.

[30] Z. Wu, H. Zhong, X. Yuan, H. Wang, L. Wang, X. Chen, G. Zeng, Y. Wu, Reply for comment on "adsorptive removal of methylene blue by rhamnolipid-functionalized graphene oxide from wastewater", Water Res., 67 (2014) 330–344.

[31] Q. Wu, H. Zhang, L. Zhou, Synthesis and application of RGO/coFe_2O_4, composite for catalytic degradation of methylene blue on heterogeneous Fenton-like oxidation, J. Taiwan Inst. Chem. E., 67 (2016) 484–494.

[32] S.S. Lin, M.D. Gurol, Catalytic decomposition of hydrogen peroxide on iron oxide: kinetics, mechanism, and implications, Environ. Sci. Technol., 32 (1998) 1417–1423.

[33] X.C. Wang, J.Y. Wu, H.P. Zhou, Synthesis, crystal structures and electrochemical properties of two new metal-centered ferrocene complexes, Sci. China Chem., 52 (2009) 930–993.

[34] B. Yang, Z. Tian, L. Zhang, Enhanced heterogeneous Fenton degradation of methylene blue by nanoscale zero valent iron (nzvi) assembled on magnetic Fe_3O_4 /reduced graphene oxide, J. Water Proc. Eng., 5 (2015) 101–111.

[35] W.X. Wang, K.J. Xiao, L. Zhu, Y.R. Yin, Z.M. Wang, Graphene oxide supported titanium dioxide & ferroferric oxide hybrid, a magnetically separable photocatalyst with enhanced photocatalytic activity for tetracycline hydrochloride degradation, RSC Adv., 7 (2017) 21287–21297.

[36] M.A. Voinov, J.O. Sosa Pagán, E. Morrison, T.I. Smirnova, A.I. Smirnov, Surface-mediated production of hydroxyl radicals as a mechanism of iron oxide nanoparticle biotoxicity, J. Am. Chem. Soc., 133 (2011) 35–41.

[37] L.J. Xu , J.L. Wang, A heterogeneous Fenton-like system with nanoparticulate zero-valent iron for removal of 4-chloro-3-methyl phenol, J. Hazard. Mater., 186 (2011) 256–264.

[38] J. Yan, M. Lei, L. Zhu, M.N. Anjum, J. Zou, H. Tang, Degradation of sulfamonomethoxine with Fe_3O_4 magnetic nanoparticles as heterogeneous activator of persulfate, J. Hazard. Mater., 186 (2011) 1398.

[39] W.G. Kuo, Decolorizing dye wastewater with Fenton's reagent, Water Res., 26 (1992) 881–886.

[40] X.R. Xu, X.Z. Li, Degradation of azo dye orange g in aqueous solutions by persulfate with ferrous ion , Sep. Purif. Technol., 72 (2010) 105–111.

[41] H. Hassan, B.H. Hameed, Fe–clay as effective heterogeneous Fenton catalyst for the decolorization of reactive blue 4, Chem. Eng. J., 171 (2011) 912–918.

[42] Y. Liu, H. Zhang, Y.F. Lu, J. Wu, B.F. Xin, A simple method to prepare g-c3n4/ag-polypyrrole composites with enhanced visible-light photo-catalytic activity, Catal. Commun., 87 (2016) 41–44.

[43] C. Bao, H. Zhang, L.C. Zhou, Y.M. Shao, J.J. Ma, Q. Wu, Preparation of copper doped magnetic porous carbon for removal of methylene blue by a heterogeneous Fenton-like reaction, RSC Adv., 5 (2015) 72423–72432.

[44] J.K. Du, J.G. Bao, X.Y. Fu, C.H. Lu, S.H. Kim, Mesoporous sulfur-modified iron oxide as an effective Fenton-like catalyst for degradation of bisphenol a, Appl. Catal. B: Environ., 184 (2016) 132–141.

[45] R.J. Wang, X.Y. Liu, R.H. Wu, B.W. Yu, TiO_2-doped Fe_3O_4 nanoparticles as high-performance Fenton-like catalyst for dye decoloration, RSC Adv., 6 (2016) 8594–8600.

[46] K. Dutta, S. Mukhopadhyay, S. Bhattacharjee, B. Chaudhuri, Chemical oxidation of methylene blue using a Fenton-like reaction, J. Hazard. Mater., 84 (2001) 57–71.

[47] G.V. Buxton, C.L. Greenstock, W.P. Helman, A.B. Ross, Critical review of rate constants for reactions of hydrated electrons chemical kinetic data base for combustion chemistry. part 3: propane, J. Phys. Chem. Ref. Data, 17 (1988) 513–886.

[48] A. Long, Y. Lei, H. Zhang, Degradation of toluene by a selective ferrous ion activated persulfate oxidation process, Ind. Eng. Chem. Res., 53 (2014) 1033–1039.

[49] C. Wang, J. Kang, H.Q. Sun, H.M. Ang, M.O. Tad, S.B. Wang, One-pot synthesis of N-doped graphene for metal-free advanced oxidation processes, Carbon, 102 (2016) 279–287.

[50] W. Songlin, Z. Ning, Removal of carbamazepine from aqueous solution using sono-activated persulfate process, Ultrasonics Sonochemistry, 29 (2016) 156–162.

[51] W. Liu, J. Ma, C. Shen, Y. Wen, W. Liu, A ph-responsive and magnetically separable dynamic system for efficient removal of highly dilute antibiotics in water, Water Res., 90 (2016) 24–33.

[52] J.H. Ramirez, C.A. Costa, L.M. Madeira, G. Mata, M.A. Vicente, M.L. Rojas-Cervantes, Fenton-like oxidation of orange ii solutions using heterogeneous catalysts based on saponite clay, Appl. Catal. B: Environ., 71 (2007) 44–56.

[53] J. Deng, J. Jiang, Y. Zhang, X. Lin, C. Du, Y. Xiong, $FeVO_4$, as a highly active heterogeneous Fenton-like catalyst towards the degradation of orange ii, Appl. Catal. B: Environ., 84 (2008) 468–473.

[54] S.S. Lin, M.D. Gurol, Catalytic decomposition of hydrogen peroxide on ironoxide: kinetics, mechanism, and implications, Environ. Sci. Technol., 32 (1998) 1417–1423.

[55] W.P. Kwan, B.M. Voelker, Decomposition of hydrogen peroxide and organic compounds in the presence of dissolved iron and ferrihydrite, Environ. Sci. Technol., 36 (2002) 1467–1476.